Department of Veterans Affairs

Journal of Rehabilitation Research and Development Vol. 35 No. 2, June 1998
Pages 161–176

Material properties of commonly-used interface materials and their static coefficients of friction with skin and socks

Joan E. Sanders, PhD; Joan M. Greve, BSBE; Stuart B. Mitchell, BSME; Santosh G. Zachariah, PhD
Department of Bioengineering, University of Washington, Seattle, WA 98195

Abstract—Compressive stiffness (CS) of different supporting materials used in prosthetics and orthotics and their static coefficients of friction (COF) with skin and socks were characterized. Materials tested included Spenco, Poron, nylon-reinforced silicone, Soft Pelite, Medium Pelite, Firm Plastazote, Regular Plastazote, and Nickelplast. A displacement-controlled testing device was constructed to assess the CS of 11.1 mm diameter material specimens under cyclic loading (1 Hz) to 220 kPa over 10- and 60-min periods. Results demonstrated local CS ranging from 687 kPa (Poron) to 3,990 kPa (Soft Pelite). To fit the cyclic stress-strain (S-S) data within an error of 4.0 percent full-scale output, the minimum order of fit required for Spenco, Poron, and nylon-reinforced silicone was a third-order polynomial; for Soft Pelite, Medium Pelite, Firm Plastazote, and Regular Plastazote, a second-order polynomial; and for Nickelplast, a linear fit. For all materials, the nonrecovered strains were related to loading time using an exponential fit. A biaxial force-controlled load applicator device was used to assess COF at skin-material, sock-material, and skin-sock interfaces for shear forces of 1 to 4 N applied to a 10.2×7.8 mm loading pad. COFs ranged from 0.48 (±0.05) to 0.89 (±0.09). COFs at skin-material interfaces were significantly ($p<0.05$) higher than those at skin-sock interfaces. There was a trend of a higher COF at sock-material interfaces than at skin-sock interfaces. These data are of potential utility in finite element modeling sensitivity analysis of residual limb-prosthetic socket systems or body-orthosis systems to characterize effects of material features on interface pressure and shear stress distributions.

Key words: *amputation, friction, interface materials, interface stress, orthotics, prosthetics, shoe inserts.*

INTRODUCTION

The distribution of mechanical stress at body support interfaces can influence the risk of tissue breakdown. Excessive pressure and shear stress can lead to skin blisters, cysts, or ulceration. Interface materials influence the pressure and shear distribution on skin and underlying tissues principally via their elastic properties and their frictional characteristics with skin. An important elastic property is the compressive stiffness (CS), the instantaneous slope of the stress-strain (S-S) curve under compression loading. Low CS interface materials attenuate stress concentrations associated with bony prominences. A relevant frictional characteristic is the static coefficient of friction (COF), the ratio of shear force to normal force necessary to initiate movement of the material relative to the skin. Thus, a material with a low COF with skin will induce low shear stresses. Though a low CS material that also has a low COF with skin may be very safe in terms of minimizing risk of tissue breakdown, it can be unsafe because of a lack of adequate mechanical coupling between the soft tissues and the supporting device (prosthesis, orthosis). Individuals with amputations using such materials to line their prostheses, for example, could be unstable and fall. A challenge in materials selection is to choose materials

This material is based upon work supported, in part, by the National Institute of Child and Human Development of the National Institutes of Health.

Address all correspondence and requests for reprints to: J.E. Sanders, PhD, Associate Professor, Department of Bioengineering, Box 357962, Harris Hydraulics 309, University of Washington, Seattle, WA 98195; email: sanders@limbs.bioeng.washington.edu.

that are somewhere between the two extremes, providing an interface pressure and shear stress distribution that induces adequate stability but not an excessive risk of tissue breakdown.

Several investigators have quantified the CS of interface materials used in prosthetics and orthotics. Campbell (1) evaluated 31 different materials used mainly for shoe inserts to a maximal stress of 353 kPa, applied at a 10 mm/min strain rate. They concluded that, based on their S-S curves, the materials could be divided into three groups: very stiff, moderately deformable, and highly deformable. However, no quantitative criteria were given for dividing the groups; only a qualitative description of their S-S curves was used. Those studies were then extended (2) to investigate the effects of heat, sustained loading, and repetitive loading on the material "log standardized strain." The log standardized strain was defined at a specified stress as the log of the ratio of strain of the material subjected to the service condition to the strain of the virgin material. The resulting log standardized stress plots were used to group most of the materials into the three categories. Sanders (3) loaded specimens of Pelite, a closed-cell polyethylene foam commonly used in prosthetics, cyclically at 1 Hz to 200 kPa, characterized the resulting S-S curve as bi-phasic, fitting one slope to the low strain portion (0 to 80 kPa) and one slope to the high strain (80 to 200 kPa) portion of the curve. Kuncir (4) describes compression studies where an exponential was used to fit compression testing S-S data for selected polyethylene foams; however, the specimen size, protocol, and error in the fit were not given. Others did not evaluate the shape of the S-S curve, but instead compared thickness before and after loading. Brodsky (5) found that some shoe insert materials subjected to combined compression and shear cyclic loading recovered better than specimens subjected to just compression at the same stress level. Kuncir (4) loaded materials in a static testing apparatus, then evaluated their recovery after 1 wk of continuous loading. Orders (6) evaluated thickness changes in Plastazote insoles used by subjects for 12 wks. Thus, compression-testing studies reported in the literature have tended to concentrate on characterization of the recoverable portions of S-S curves or of plastic deformations after loading. Evaluation of the nonrecovered strain during repetitive loading has not been reported. Only one report (4) discusses nonlinear curve-fitting of the S-S data. Thus, for sensitivity analyses where quantitative characterization of the complete compressive responses of interface materials is needed, the data currently available in the literature are incomplete.

A number of devices to measure static COF have been developed, mainly for ergonomic research applications where the interest is at the shoe-walking surface interface. Over 60 different meter devices (7) have been developed for the assessment of COF for this application. Inclined planes, motor-driven sleds (8), and custom-designed machines (9) to apply loads to a shoe on a flat surface have been used to measure COF. Test results show that static COF is highly sensitive to a number of factors, including the presence of contaminants on the surface (10), initial velocity (8), and time of contact (11). Andres proposed that sensitivity to time of contact is explained by the buildup of an adhesion force between the two surfaces that increases the COF over time (12).

COF has also been measured at skin-material interfaces. Naylor (13) designed a motor-driven loading device to investigate COF between polyethylene and skin over the middle third of the anterior tibial region. He applied loads at 0.33 Hz to a maximum of 127 kPa normal stress (assuming a uniformly-distributed load). Data for one subject showed that dry skin had a COF with polyethylene of approximately 0.6. Sweat increased COF to 1.0, but when air was blown over the surface it went down to 0.8. COF also decreased when the skin surface was flooded with water. Cleaning the skin with ether increased COF to between 0.8 and 1.1, while adding oil decreased COF.

Comaish (14) suggested that static COF was nonlinearly dependent on the magnitude of the applied force. He used a slip threshold test to demonstrate that, in general, this was true. Comaish found that when a hand was immersed in water for 30 min then dried, the COF increased, both for a wool and a teflon contacting surface, suggesting that hydration of the stratum corneum influenced COF. COF on the palm was greater than that on the dorsum of the hand.

Other investigators measured dynamic COF instead of static, using a rotating wheel that contacted the skin surface (15–17). On the middle third of the volar forearm, Elsner (15) found that with a teflon contacting surface, COF on postmenopausal women was 0.45 ($\pm$0.01) while on premenopausal women it was 0.49 ($\pm$0.02). Dynamic COF on the vulva was approximately 0.66 ($\pm$0.03), supporting the hypothesis that skin friction increased with hydration of the stratum corneum. Cua (16) found no significant difference between young and old subjects, though a dependence

on body location was demonstrated. Dynamic COF values ranged from 0.12 (±0.01) on the abdomen to 0.34 (±0.02) on the forehead and postauricular. Highley (17) explained that dynamic COF increased when a small amount of water was put on the surface, because the water encouraged adhesion of stratum corneum cells to the contacting surface. Oil reduced the dynamic COF via hydration and inhibition of this sticky effect.

Thus, COF investigations to date have provided insight and quantitative data, but they have been limited to surfaces much stiffer than interface materials for rehabilitation applications, excluding Comaish's study on wool. Assessment of interface materials used in prosthetics and orthotics, has not been reported nor a comparison among materials conducted.

The purpose of this research was to build on previous studies to characterize: 1) the time-dependent S-S response of commonly used interface materials; 2) COFs between skin and interface materials, skin and a wool sock, and a wool sock and interface materials.

METHODS

Materials

Eight materials underwent compression testing: Spenco, Poron, nylon-reinforced Silicone, Soft Pelite, Medium Pelite, Firm Plastazote (LD70), Medium Plastazote (LD45), and Nickelplast. Common uses of these materials in prosthetics and orthotics are described in **Table 1.** With the exception of nylon-reinforced Silicone and Soft Pelite, the same types of materials were evaluated for their COFs with the skin of human volunteers. Nylon-reinforced Silicone was not tested because it tended to crack during shear loading. Soft Pelite was not tested because it became extremely thin after short-term loading; thus, the results were extremely sensitive to the angle of the loading device with the skin. Additional studies were conducted to evaluate COF at skin-wool sock interfaces as well as at wool sock-material interfaces for the same six materials used for COF testing. All materials were obtained through a common distributor (Knit-Rite Incorporated, OBP Distributors, Kansas City, MO) in thickness as near to 4.0 mm as were available. All materials were of condition received from the distributor. Cross sections of these materials are shown in **Figures 1a** through **1h.**

Compression Testing

A computer-controlled compression testing apparatus was designed and constructed to apply repeated sinusoidal normal displacements to 11.1 mm disks of material. This test was similar to ASTM standards test number D3574-91 test C (*Standard test methods for flexible cellular materials: Compressive force test*) except the specimen size was smaller, the bottom platen was not perforated, the loading rate was 1.0 Hz, not 0.083 Hz, and the maximum stress was approximately 220 kPa, not 140 Pa. The load rate and maximum stress were changed to better reflect the conditions encountered in a socket, orthosis, or shoe during ambulation (18). The specimen diameter:thickness ratio was approximately the same as that of the standard (2.8:1). The compression-testing device was designed so that

Table 1.
Materials tested.

Material	Description	Common Uses
Spenco	silicone-based, neoprene with a fabric membrane on top	Brace liners (usually knee braces), shoe insert liners, shoe inserts
Poron	open-cell urethane foam but according to the manufacturer it does not let moisture through	Shoe inserts, shoe insert liners
Silicone	nylon-reinforced, silicone-based	Below-knee socket inserts (custom made or off the shelf) and distal end caps; shoe inserts
Soft Pelite	closed-cell polyethylene foam	Padding for braces (usually ankle foot orthoses), particularly at the edges
Medium Pelite	closed-cell polyethylene foam	Below-knee socket inserts
Firm Plastazote	closed-cell crosslinked polyethylene foam	Spinal brace liners
Regular Plastazote	closed-cell crosslinked polyethylene foam	Soft distal end caps for below-knee and above-knee sockets; diabetic shoe inserts
Nickelplast	closed-cell polyethylene foam, alloy of ethylene vinyl acetate	Below-knee socket inserts

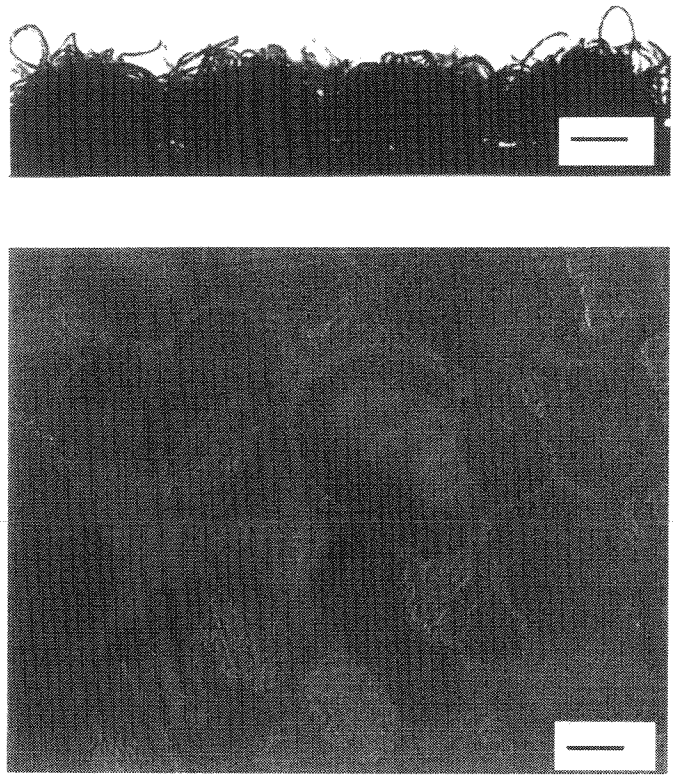

Figure 1a.
Cross section of Spenco. In **Figures 1a** through **1h,** cross-sectional planes perpendicular to the surface that contacted the skin are shown. Sections were cut to 0.25 to 0.50 mm thickness and were photographed under a light microscope at a magnification that provided the greatest insight into the structure. Upper panel: cross section at the surface, bar=200 μm. Lower panel: cross section through the mid-region, bar=50 μm.

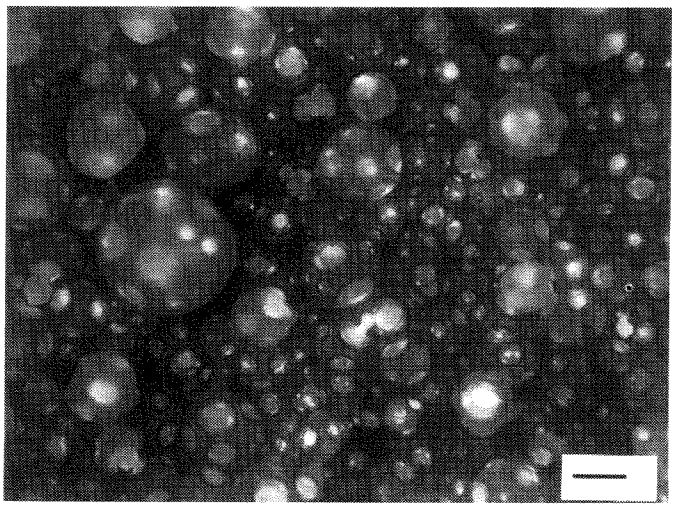

Figure 1b.
Cross section of Poron; bar=100 μm.

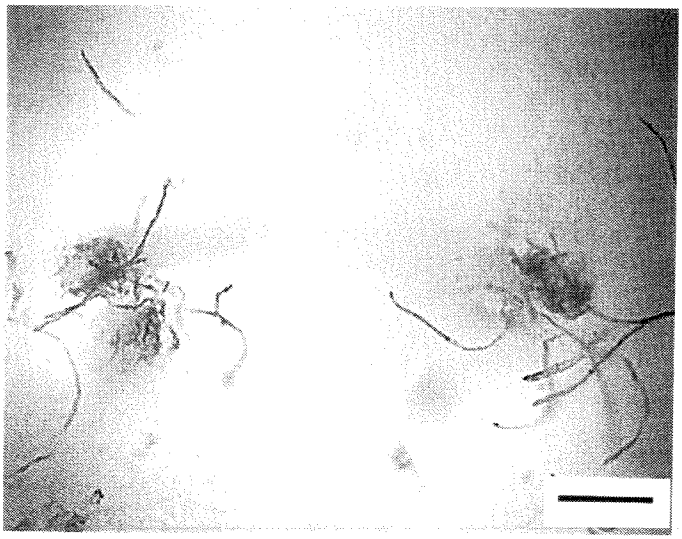

Figure 1c.
Cross section of nylon-reinforced Silicone; bar=100 μm.

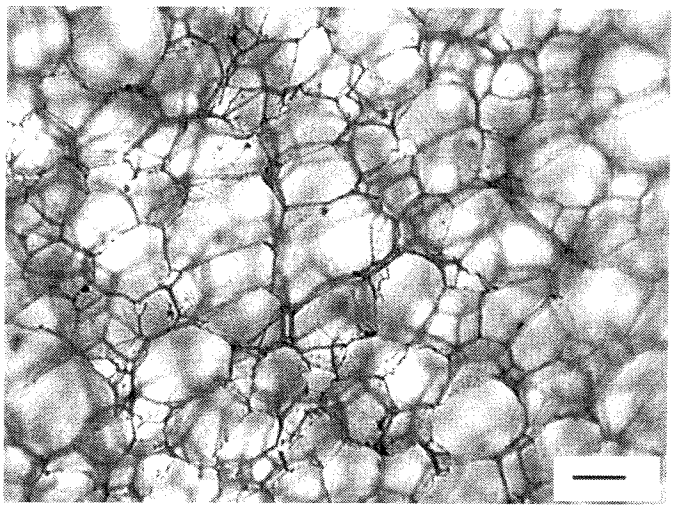

Figure 1d.
Cross section of Soft Pelite; bar=100 μm.

the axis of a shaker motor (ET126/PA118, LabWorks, Costa Mesa, CA) was put in series with two U-joints with orthogonal axes, a loading rod, a linear bearing (base), an upper platen, the material specimen, a lower platen, and a load cell as shown in **Figure 2.** The maximal motor displacement was 1.91 cm. A linear variable differential transformer (LVDT; MHR500, Schaevitz, Pensauken, NJ) was used to measure displacement, with the core mounted to an arm on the face of the motor and the bore mounted to the frame of the

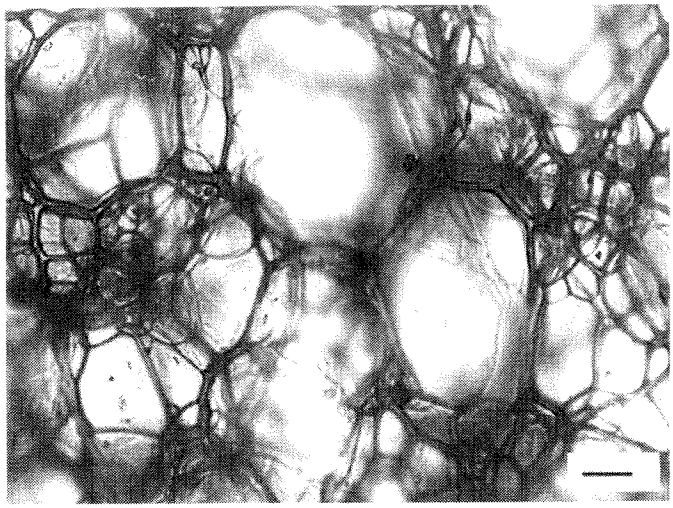

Figure 1e.
Cross section of Medium Pelite; bar=100 μm.

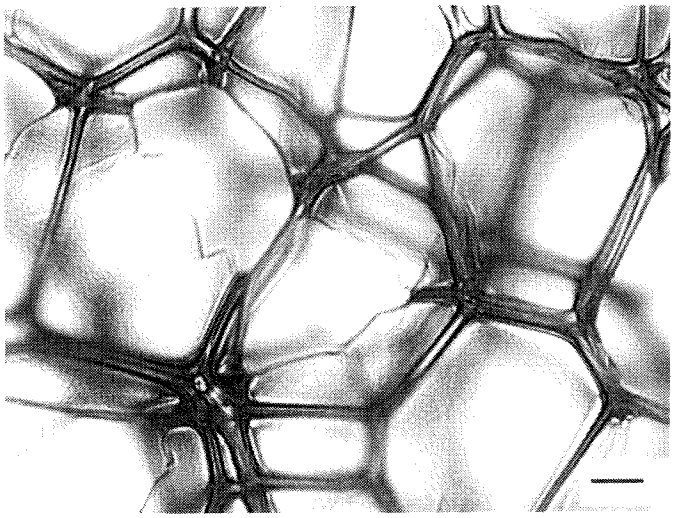

Figure 1f.
Cross section of Firm Plastazote; bar=100 μm.

testing apparatus. The material to be tested rested on a load cell (Model 41, Sensotec, Columbus, OH). Signals from the load cell were amplified (Model 2310, Measurements Group Inc., Raleigh, NC) at a gain of 500 and conditioned with a two-pole Butterworth low-pass filter with a cut-off frequency of 1,000 Hz to eliminate radio frequency noise. A Labview II (National Instruments, Austin, TX) virtual instrument, written on a Macintosh computer (Centris 650, Apple, Cupertino, CA) with a data acquisition board (NB-MIO-16, National Instruments, 409.6 bits/V) was used to apply controlled sinusoidal displacements at 1.0 Hz to the specimen while recording the force from the load cell and displacement from the LVDT at a sampling rate of 49 Hz. A 49 Hz sampling rate was determined appropriate based from spectral analysis of preliminary data. Compression testing at 1.0 Hz with no low-pass filter present and a sampling rate of 1000 Hz on Spenco demonstrated that 99.8 percent of the signal was contained within a 0 Hz to 24 Hz frequency range. A sinusoidal displacement of 1 Hz was used because this

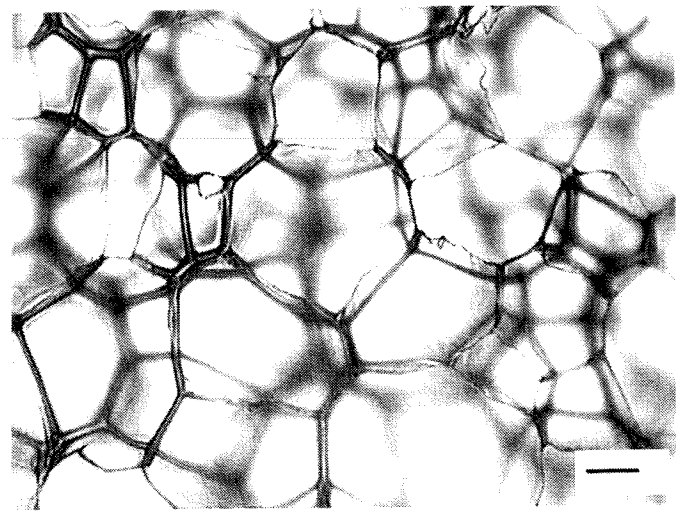

Figure 1g.
Cross section of Regular Platazote; bar=100 μm.

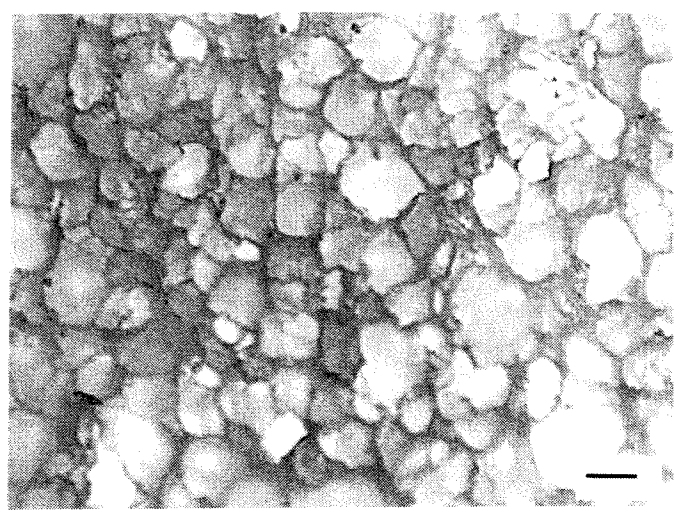

Figure 1h.
Cross section of Nickelplast; bar=100 μm.

is an approximate step rate for walking. Data were recorded at prescribed time intervals for different tests as described below.

Two different tests were performed using the compression testing system, a 10-min test and a 60-min test. The 10-min test was run to establish the order of the S-S curve under short-term loading and to establish the appropriate number of samples for further testing for a statistically significant analysis. Data were collected for 2.0 s, 1 min after loading was initiated and then again at 1-min intervals. For each material, the response after 1 min was used to determine the order of fit necessary to characterize stress as a function of strain such that the mean error was less than 4.0 percent of the full-scale output. The full-scale output was the maximal normal stress delivered to the material: approximately 220 kPa. First, the force-displacement data were converted to engineering S-S data and then the loading portions of the curves identified. Only the loading phases and not the unloading phases were used to fit curves. A least-squares optimization routine (Matlab, Natick, MA) established the coefficients for the fit (first, second, or third-order polynomial, power fit, or exponential). The lowest order polynomial fit necessary to achieve an error of less than 4.0 percent full-scale was used, but if a power fit or exponential were more accurate, that was used instead of a third-order polynomial. At least 72 hrs after allowing the materials to recover, 60-min cyclic compression tests were conducted, collecting data at a 49 Hz sampling rate for 2.0 s every 3 min. Specimen thickness was measured at least 168 hours after the 60-min loading session was completed. A room temperature of approximately 23.3 °C was maintained throughout the experiments.

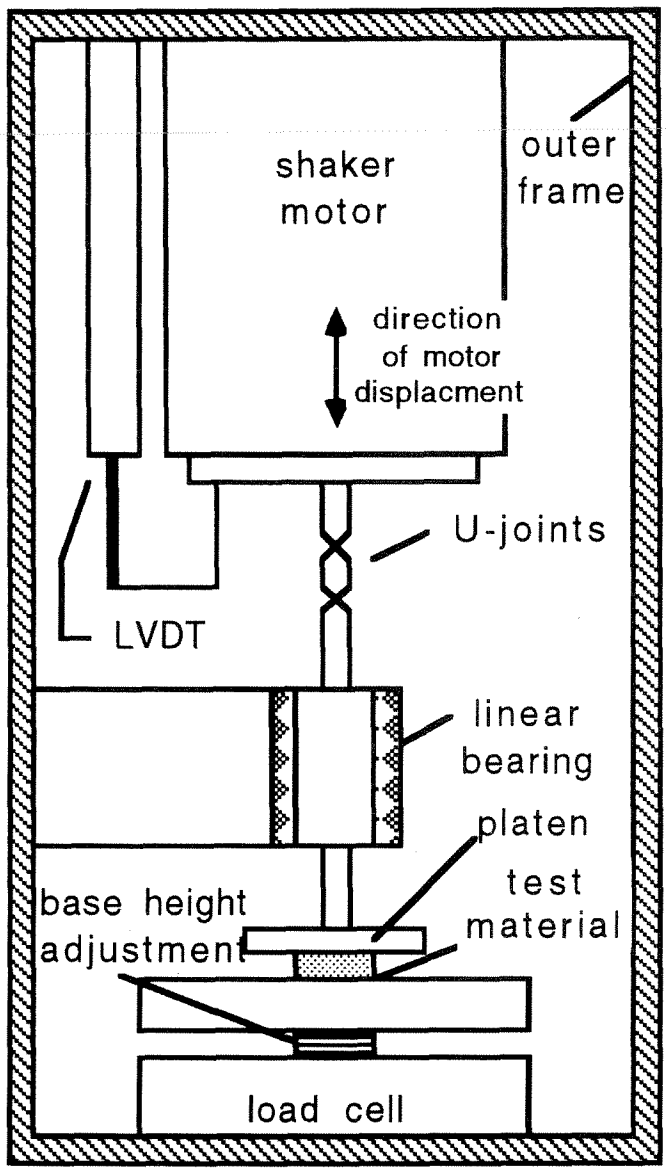

Figure 2.
Compression testing device. An 11.1 mm diameter test specimen is positioned beneath the upper platen.

A series of evaluations was carried out to establish the resolution and accuracy of the instrumentation. The load cell was calibrated with different base heights over a 1.9-cm range. Evaluation with the test load applied off-center to the outer edge of the 2.54 cm diameter upper platen was also conducted. Sensitivity to friction between the test specimen and platens was evaluated by conducting tests with a thin layer of silicone grease between the material and platens and comparing the results to those with dry interfaces.

For data from the 60-min tests, the S-S curves were divided into a Part A and a Part B, corresponding roughly to the nonrecovered and cyclic part of the S-S curve respectively (**Figure 3**). Data with compressive stress values below 3.35 kPa were put into Part A while those above 3.35kPa were put into Part B. A lower threshold would introduce curve fit problems from bit noise in the data. For the Part B portion, the least-squares optimization routine established the coefficients (A_n) for the fits in a manner similar to that used for the 10-min tests. Means of the coefficients for each 3-min period were determined and a least-squares optimization routine used to establish changes in the coefficients with respect to time. Similarly, a least-squares optimization routine was used to fit the Part A strain data with respect to time.

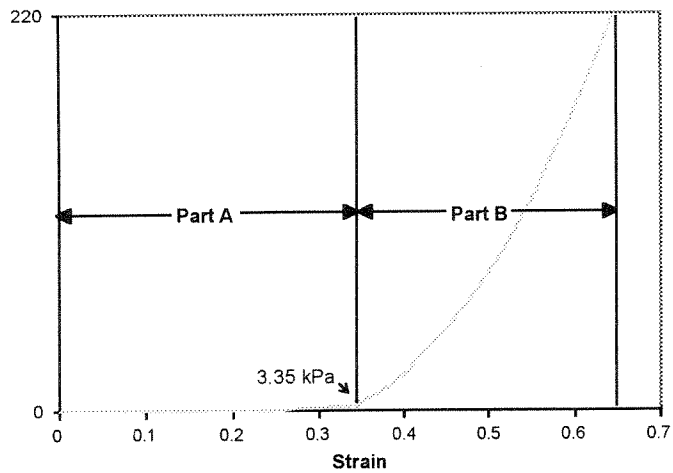

Figure 3.
Analysis of 60-min compression testing data. Stress-strain curves were divided into a Part A and Part B response. A threshold stress of 3.35 kPa marked the transition from Part A to Part B.

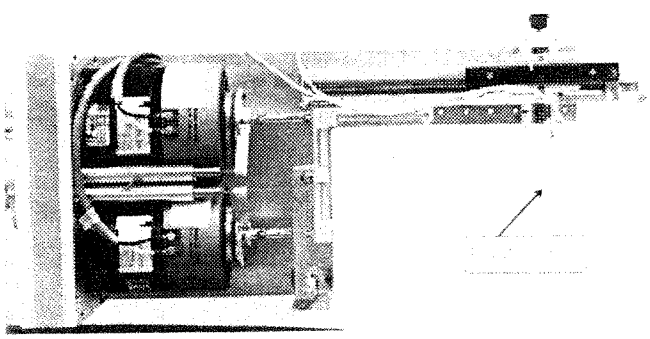

Figure 4.
Load applicator used for friction testing. The device is a closed-loop biaxial force control system. The loading pad is the contacting surface.

To determine error in the curve fits, calculated stresses were subtracted from the actual stresses and the absolute values of the results divided by the full-scale outputs. The reported error is the mean of all the errors for data from all of the time intervals for all of the samples tested for each material.

Friction Testing

The frictional testing apparatus was a bidirectional closed-loop force-control device that controlled the motion of a loading pad so as to achieve prescribed normal and shear forces at the interface of the pad with the skin. The device was used previously to investigate skin response to mechanical stress (19). Two motors (ET126/PA118, LabWorks, Costa Mesa, CA), configured in parallel, were used with a low effective mass linkage and small-angle rotational joints to deliver the force (**Figure 4**). The loading pad was a rectangular piece of the interface material to be tested. It was epoxied (DP-460, 3M, St. Paul, MN) in place to the bottom of a 10.2×7.8 mm aluminum plate on the end of the short beam of the load applicator arm. The edges of the interface material were beveled to help prevent stress concentrations in the skin near the pad edges. The digital feedback controller independently controlled the instantaneous normal and shear forces and recorded the resulting displacements. Mean absolute errors for both the normal and shear directions between the applied and reference waveforms were less than 1.2 percent full-scale.

Skin-material Interface

Testing was performed on skin on the medial tibial flare of 10 volunteer adult controls with no skin disorder, disease, or other problems. Internal review board human subjects approval was obtained for all tests. Using the level of the tibial tuberosity as a zero reference, tests were performed 3.0, 6.5, 10, and 13.5 cm distal to the reference, each site used on a different testing day to ensure that there was no overlap of testing areas. The ordering of site selection for the tests was randomly selected. To prepare a site for testing, the region was shaved with a handheld razor, cleaned with soap and warm water, and dried with a hairdryer on low heat for 10 min. A 5.0×5.0 cm patch of DuoDERM (187955 extra thin, ConvaTec, Princeton, NJ), with the central 2.2×1.9 cm removed, was placed on the skin, taking care to ensure skin tension remained the same as before this application. Then the surface of the DuoDERM was cleaned with a degreaser (CSM-1A, Measurements Group Incorporated, Raleigh, NC), a thin layer of quick-set adhesive (82307, Loctite Corporation, Cleveland, OH) was applied to the DuoDERM, and a 4.3×3.5 cm aluminum plate, 2.0 mm thick, with the central 2.3×2.0 cm removed, was put on top of the adhesive, affixing the frame to the DuoDERM (**Figure 5**). A 10 g mass was put on the center of the medial side of the frame for 10 min during curing to ensure the plate did not move while the adhesive set. The purpose of the DuoDERM and attached aluminum frame was to provide a consistent strain boundary during testing.

During testing, the subject sat on a cushion on a long table, legs extended and knees in approximately 5° of flexion, so that the aluminum frame was in a

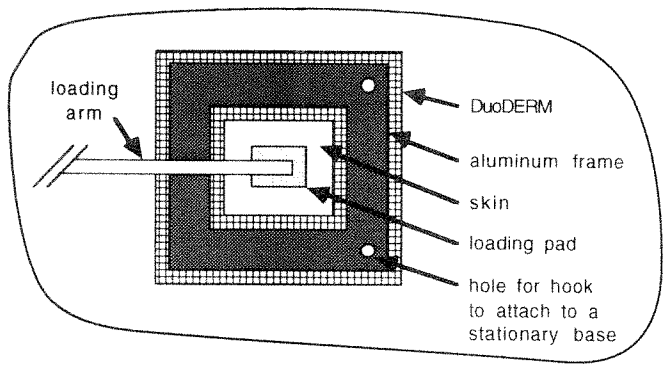

Figure 5.
Top view of friction testing region. The DuoDERM and aluminum frame helps create a uniform strain field in skin surrounding the loaded region.

horizontal plane facing upward. To ensure the frame remained stationary during load application, attachment hooks extended from holes in its edge to stationary base stands.

In each test, a repeated shear force and a stepwise decreasing normal force were applied. A cyclic, rather than a constant or linearly-increasing shear, force was used to more closely replicate the cyclic conditions at the skin-prosthesis, skin-orthosis, or skin-shoe interface encountered during walking. Five shear cycles were applied at each normal force plateau. The time at which slip occurred was apparent in the displacement data (**Figure 6**) and also was visible at the test site. A computer algorithm was written to detect slip computationally to accelerate data processing. The program compared the slopes of the motor displacement curves in successive cycles and identified slip based on a threshold difference between the two slopes. A second test was then carried out with smaller steps of normal force changes, thus enhancing the resolution of the data. Using this approach, the mean normal force resolutions for peak-to-peak shear force magnitudes of 1, 2, 3, and 4 N for all of the materials on all subjects were 0.21 (±0.03) N, 0.27 (±0.07) N, 0.36 (±0.10) N, and 0.35 (±0.12) N, respectively. Thus for each test, the normal force immediately before slip occurred and the normal force at which slip occurred spanned the actual COF value. The COF reported was the peak cyclic shear force divided by the mean of these two measurements.

To test the six materials, a total of four 2-hr sessions with 24 tests/session were required. All sessions for a subject were completed within a 7-day period. For each material at each of the four shear force levels, the high-resolution test was conducted on a different day than the low-resolution test.

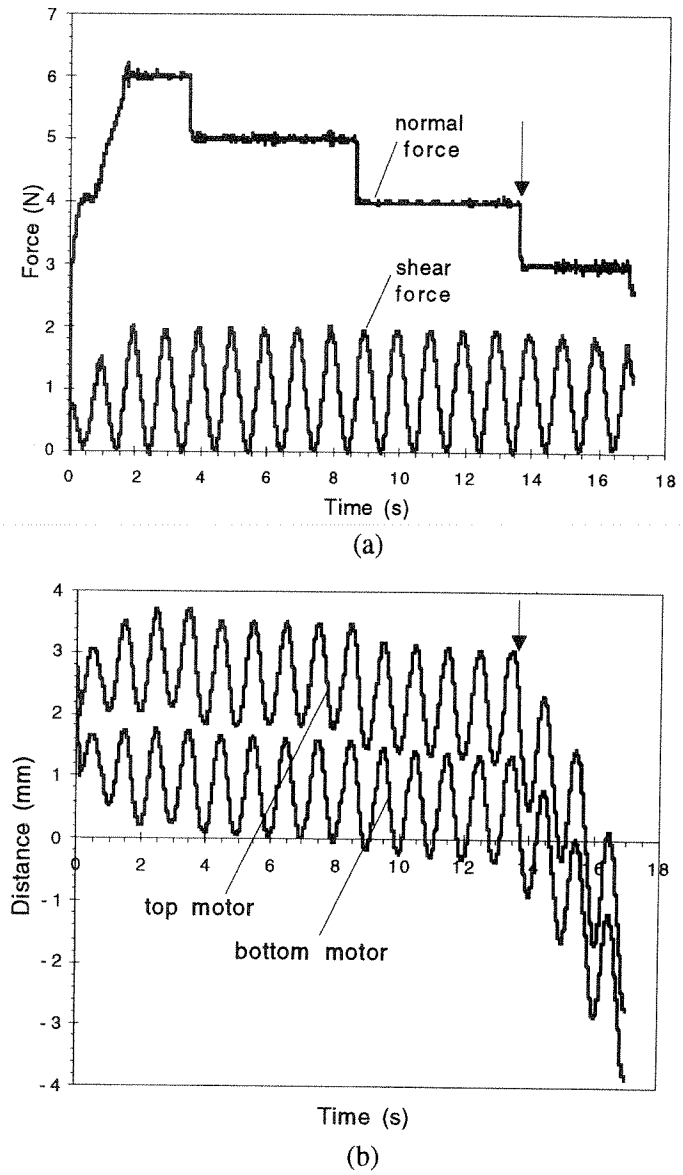

Figure 6.
Force and displacement data from a friction test: a) Normal and shear force on the loading pad; b) Displacement of the top and bottom motors. Slip occurred at the 3 N normal force level (arrow) as apparent in the displacement data.

A series of tests was carried out to establish error in the instrumentation and setup procedure. Sensitivity to surface area of the pad was evaluated by conducting tests with pads of 70 and 130 percent of the surface area of the original pad. The tests were conducted on a skin-like model described below. Sensitivity to 1 and 5°

angular deviations of the loading pad relative to the skin, both in the plane of the motor axes and in an orthogonal plane perpendicular to the skin surface, was evaluated. Repeatability error in setup angle was also conducted.

Sock-material Interface

Tests to evaluate COF between interface materials and a wool sock (3-ply OS [old style] wool sock #0, Knit-Rite Inc., Kansas City, MO) were conducted on a skin-like model rather than a human subject to reduce variability due to subject-to-subject differences. The model was a 10.0×11.5 cm block of Medium Pelite covered with a wool sock and placed on a 13.0×16.8 cm piece of wood. The edges of the sock were held in place with a 11.5×13.0 cm brass frame with three nails on each edge.

Testing was conducted using the same waveform shapes and protocol as described above for the skin-material tests.

Skin-sock Interface

Additional tests were conducted on 10 subjects (6 same as for the skin-material test) to evaluate COF between skin and a wool sock. The same apparatus and protocol as that for the skin-material interface tests was used, except that a 3.0×3.0 cm piece of wool sock was wrapped around the loading pad (Medium Pelite) and held in place with rubber bands covered by epoxy resin on the side of the loading pad. The epoxy did not contact the skin and did not contact the wool on the bottom of the pad.

For all statistical comparisons described in the results below, a criterion of $p<0.05$ was used.

RESULTS

Specimen mean initial thickness varied: the thinnest was Firm Plastazote with a mean thickness of 2.82 (±0.12) mm, while the thickest was Nickelplast at 5.26 (±0.14) mm (**Table 2**). Variability in thickness, defined as standard deviation/mean, was <5.00 percent for each material, except Regular Plastazote with a variability of 14.55 percent.

Compression Testing

Changes in base height, off-center load, and reduced friction at the material/platen interface had minimal effect on the CS results. At most, a 0.08 percent full-scale error occurred when the base height was changed over a 1.9 cm range. When the load was applied on the edge of the upper platen there was at most a 0.02 percent full-scale error. CS results with a thin layer of silicone grease between the material and platens showed a 0.5 to 2.6 percent full-scale error. The 2.6 percent error occurred in the 25–30 percent strain range. Otherwise, all errors were approximately 0.5 percent full-scale.

Ten-minute Tests

To fit the data within a 4.0 percent full-scale error, Spenco, Poron, and Silicone required at least a third-order polynomial; Soft Pelite, Medium Pelite, Firm Plastazote, and Regular Plastazote required at least a second-order polynomial; and Nickelplast required at least a first-order polynomial (**Table 3**). Logarithmic or exponential fits did not improve the curve-fitting errors for any of the materials. For a statistically significant analysis, a total of 16 specimens per group were necessary, thus 16 samples/group were used in the 60-min tests.

Five of the eight materials (Spenco, Poron, Soft Pelite, Medium Pelite, and Firm Plastazote) demonstrated significant decreases in specimen thickness from before the 10-min test to before the 60-min test, indicating plastic deformation occurred. However, none of the changes were greater than 5.00 percent of the original thickness; they were 1.47 (±0.49), 0.35 (±0.57), 4.60 (±0.81), 4.53 (±1.65), and 3.87 (±0.65) percent, respectively.

Sixty-minute Tests

Results from the 60-min tests showed that both the Part A and Part B response changed over time. For all

Table 2.
Specimen initial thickness (n=16).

Material	Thickness	Variability
Spenco	3.96 (±0.02)	0.51
Poron	3.18 (±0.01)	0.31
Silicone	4.22 (±0.45)	0.66
Soft Pelite	3.10 (±0.03)	0.97
Medium Pelite	3.10 (±0.05)	1.16
Firm Plastazote	2.82 (±0.12)	4.26
Regular Plastazote	3.30 (±0.48)	14.55
Nickelplast	5.26 (±0.14)	2.66

Thickness=mean±SD, in mm; variability=SD/mean, in percent.

Table 3.
Material groupings.

Group 1: $\sigma(\epsilon,t) = A_3(t)\epsilon^3 + A_2(t)\epsilon^2 + A_1(t)\epsilon$	Group 2: $\sigma(\epsilon,t) = A_2(t)\epsilon^2 + A_1(t)\epsilon$	Group 3: $\sigma(\epsilon,t) = A_1(t)\epsilon$
Spenco	Soft Pelite	Nickelplast
Poron	Medium Pelite	
Silicone	Firm Plastazote	
	Regular Plastazote	

Table 4.
Coefficients for Part A from the 60-minute tests.

Group	Material	X	Y	Fit Error
1	Spenco	0.0779	0.1973	7.27±6.01
	Poron	0.0906	0.0489	28.47±14.15
	Silicone	0.3716	0.0392	10.97±7.49
2	Soft Pelite	0.3882	0.2147	2.36±1.79
	Medium Pelite	0.2252	0.1838	5.93±5.42
	Firm Plastazote	0.1851	0.2067	5.51±7.55
	Regular Plastazote	0.2538	0.2101	4.77±4.39
3	Nickelplast	0.0610	0.1196	13.96±10.71

Fit error=mean±SD, as % FSO; $\epsilon=Xt^Y$; t is in minutes.

materials, 50 percent of the total Part A strain was achieved within the first 3 min of the test. Thickness 1 hr after completion of the 60-min tests varied considerably (**Figure 7**). An exponential fit to the Part A strain data as a function of time achieved a mean error of less than 7.3 percent full-scale for Spenco, Soft Pelite, Medium Pelite, Firm Plastazote, and Regular Plastazote (**Table 4**). Fit errors for Poron and Nickelplast were considerably higher than for the other materials; however, their total Part A strains were much smaller. The Silicone tended to stick to the platens during testing, causing force measurement error and noise in the data, resulting in a mean Part A strain fit error of 10.97 (±7.49) percent full-scale.

Though there was appreciable deformation over the 60-min tests, all the materials except Soft Pelite (**Figure 7**) recovered well afterward. At least 1 wk after testing, Soft Pelite had a mean decrease in thickness of 2.9 (±1.0) percent. Nonrecovered strains for the Group 2 materials were consistently greater than those for Group 1 or 3 materials.

The Part B response of the S-S curves also changed as a function of time, altering the coefficients required to fit the data. Typically, the curves developed a steeper slope in their high-strain portions. The exception was Nickelplast, which showed a slightly shallower slope over time. Fit errors for just the Part B S-S response were less than 8.70 percent full-scale for all materials except Silicone and Soft Pelite, 14.69 (±19.75) and 18.89 (±24.10) percent full-scale, respectively (**Table 5**).

Table 5.
Coefficients for Part B from the 60-minute tests for each of the groupings listed in Table 3.

Group	Material	A_3	A_2	A_1	Fit Error
1	Spenco	$-0.7369t^2 + 64.787t + 3340.1$	$0.3361t^2 - 22.542t - 1429.7$	$-0.0322t^2 + 1.8005t + 412.91$	5.37 ± 5.72
		$-0.0364t^2 + 4.7827t + 3067.8$	$0.0137t^2 - 1.6117t - 2100.5$	$-0.0011t^2 - 0.0416t + 644.2$	2.53 ± 2.19
	Silicone	$81.231t + 17191$	$0.1032t^2 - 12.568t - 4364.6$	$-0.0068t^2 + 0.5931t + 586.99$	14.69 ± 19.75
2	Soft Pelite		$5.0525t^2 + 177.63t + 1374.8$	$2.4361t^2 - 47.099t + 202.9$	18.89 ± 24.10
	Medium Pelite		$46.954t + 1194.8$	$-0.0052t^2 + 0.4293t + 211.63$	6.17 ± 4.41
	Firm Plastazote		$29.003t + 1531.0$	$0.0279t^2 - 0.4773t + 290.36$	5.74 ± 4.68
	Regular Plastazote		$70.862t + 969.57$	$0.0367t^2 - 1.8717t + 67.689$	8.68 ± 7.49
3	Nickelplast			$0.0448t^2 - 5.0957t + 1455.8$	6.52 ± 5.11

Fit error=mean±SD, as % FSO; t is time in minutes.

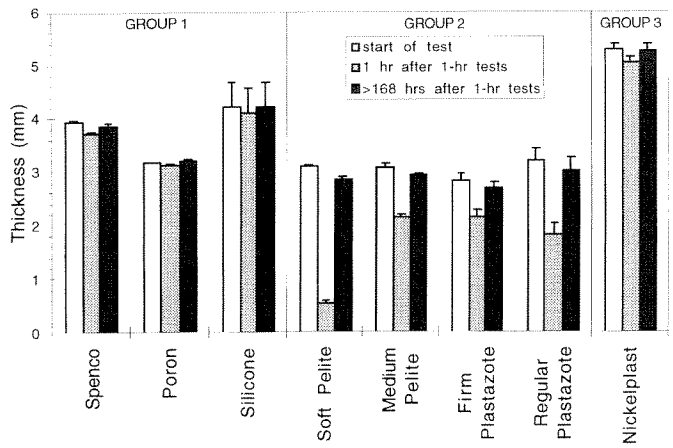

Figure 7.
Specimen thickness at three time points are shown: the start of the study, 1 hr after the 60-min compression tests, and more than 168 hours after the 60-min compression tests.

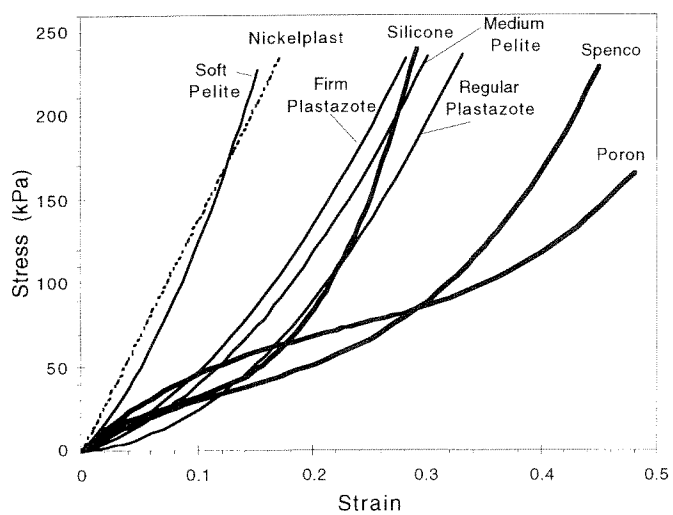

Figure 8.
Stress-strain curve fits for data collected 15 minutes into the 60-minute compression testing experiments. Only Part B data are shown. Group 1: thick lines. Group 2: thin lines. Group 3: dashed line.

The shapes of Part B of the S-S curves varied considerably among the different materials, resulting in a wide range of CS. Typical S-S results at the 15-min mark are illustrated in **Figure 8.** Over the 60-min loading session, the minimum local CS among all materials was 687 kPa (Poron) while the maximum was 3990 kPa (Soft Pelite). Local CS is the instantaneous slope of the S-S curve.

Table 6.
Curve-fitting errors for entire curves.

Group	Material	Fit Error
1	Spenco	6.58 ± 6.09
	Poron	6.97 ± 5.31
	Silicone	20.81 ± 20.49
2	Soft Pelite	25.32 ± 25.04
	Medium Pelite	13.15 ± 11.14
	Firm Plastazote	12.12 ± 9.89
	Regular Plastazote	11.83 ± 13.87
3	Nickelplast	9.17 ± 9.65

Fit error=mean±SD, as % FSO.

The Part A equations (**Table 4**) and the Part B equations (**Table 5**) can be used together to calculate a S-S response for a material after a specified loading-time interval. The nonrecovered strain (Part A) at the specified time is calculated then added to the Part B stress calculation, shifting the S-S curve away from the origin. Error, defined as the difference between the actual stress and that calculated from the equations divided by the full-scale output, ranged from 6.58 (±6.09) for Spenco to 25.32 (±25.04) percent full-scale for Soft Pelite (**Table 6**). Errors for the combined Part A and Part B responses were greater than those for the Part A and Part B portions separately, because slight errors in the Part A strain calculations caused large errors in the total stress calculations. In other words, the location of the transition point from Part A to Part B was highly sensitive to the Part A strain calculation.

Friction Testing

COF data collected on the skin model with loading pads of dimensions 70 and 130 percent of the original pad surface area did not show significant differences in COF compared with that of the original pad. Repeatability tests demonstrated that the pad could be consistently positioned within a 1° angle in any direction without the COF results changing significantly.

Skin-material Interface

In approximately 15 percent of the 210 tests conducted at shear force levels of 3 N and 4 N, day 2 COF results (high resolution) were inconsistent with those from day 1 (low resolution). In 13 of 18 such cases, the COF from day 2 was higher. These differences were expected to be due to the loading history: maximal normal forces applied on day 1 were higher, possibly causing release of fluid from skin cells or

Table 7.
Frictional coefficients at the skin-material interface.

Shear Force (N)	Spenco	Poron	Medium Pelite	Firm Plastazote	Regular Plastazote	Nickelplast
1	0.66 ± 0.10	0.75 ± 0.11	0.62 ± 0.05	0.74 ± 0.08	0.67 ± 0.08	0.73 ± 0.12
2	0.60 ± 0.05	0.75 ± 0.10	0.69 ± 0.09	0.75 ± 0.08	0.73 ± 0.09	0.82 ± 0.10
3	0.72 ± 0.11	0.69 ± 0.04	0.77 ± 0.10	0.82 ± 0.12	0.78 ± 0.12	0.83 ± 0.11
4	0.80 ± 0.08	0.77 ± 0.06	0.83 ± 0.11	0.89 ± 0.09	0.83 ± 0.08	0.83 ± 0.10
all force levels	0.69 ± 0.11	0.74 ± 0.08	0.73 ± 0.12	0.80 ± 0.11	0.75 ± 0.11	0.80 ± 0.11

Mean±SD.

Table 8.
Frictional coefficients at the sock-material interface.

Shear Force (N)	Spenco	Poron	Medium Pelite	Firm Plastazote	Regular Plastazote	Nickelplast
1	0.63	0.84	0.60	0.63	0.63	0.75
2	0.60	0.69	0.55	0.60	0.58	0.69
3	0.67	0.75	0.55	0.65	0.57	0.69
4	0.84	0.88	0.68	0.68	0.69	0.69
all force levels	0.69	0.79	0.60	0.64	0.62	0.71

altering the underlying tissue properties. In cases where there was a discrepancy between results, the normal force threshold was taken as the mean of the lower bound for the day 1 results and the lower bound for the day 2 results; thus, the day 2 results were weighed more heavily in this calculation. Results from the low shear force tests (1 N and 2 N) did not show differences in COF data for day 2 that were outside the range established in day 1, thus no correction was necessary for those data.

In general, the normal force versus shear force curves were nonlinear, and the COF increased with higher applied force (**Table 7**). The COF ranged from 0.60 (±0.05) for Spenco at 2 N shear force to 0.89 (±0.09) for Firm Plastazote at 4 N shear force. For data from the same material, COF magnitudes at a shear force of 1 N were significantly lower from those at 4 N shear force for all materials except Poron.

The standard deviations in the data (**Table 7**) suggest subject-to-subject variability in COF values. However, no subject consistently displayed higher or lower COFs than other subjects at all shear force levels for all materials.

There were significant differences in COF magnitudes for different materials; however, the differences were not consistent across all force levels (**Figure 9**). At low shear force (2 N) Spenco demonstrated significantly lower COFs compared with the other materials, while Nickelplast showed significantly higher COFs compared with the other materials. A paired t-test was used to make the comparisons shown in **Figure 9.** At high shear forces (3 N and 4 N), Poron tended to have lower COFs compared with the other materials.

When differences in COF magnitudes between material groups established from compression testing were considered, there were differences among the three groups. In general, stiffer materials had higher COF values. Group 3 (Nickelplast) COF values were higher than those of Group 2 (Regular Plastazote, Firm Plastazote, and Medium Pelite) as well as those from Group 1 (Poron, Spenco). Group 2 COF values tended to be higher than those for Group 1 (**Figure 9**).

Sock-material Interface

The curves for normal force vs. shear force were nonlinear, and COF values were higher for 1 N and 4 N shear force than for 2 N and 3 N. COF values ranged from 0.55 for Medium Pelite at 2 and 3 N to 0.88 for Poron at 4 N (**Table 8**). There was a trend of higher COF values for Group 1 materials than for Group 2 materials.

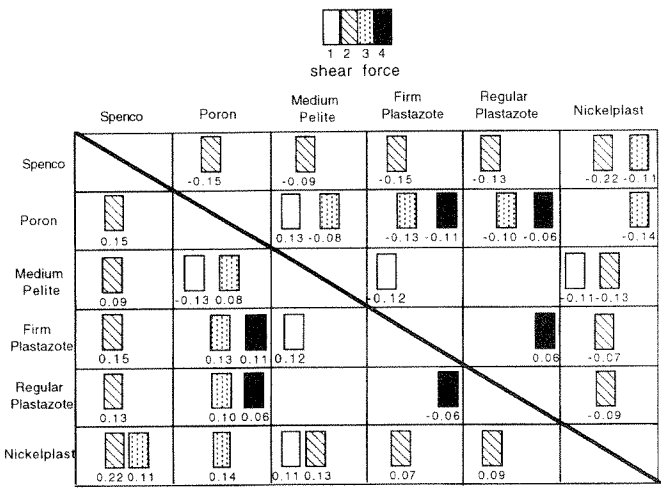

Figure 9.
Differences in COF at the skin-material interface among different materials. Each pair of materials is compared. A symbol indicates a significant difference at that shear force level and the number beneath is the magnitude difference in the COF values between the two materials. A positive difference indicates that the row has a greater COF than the column.

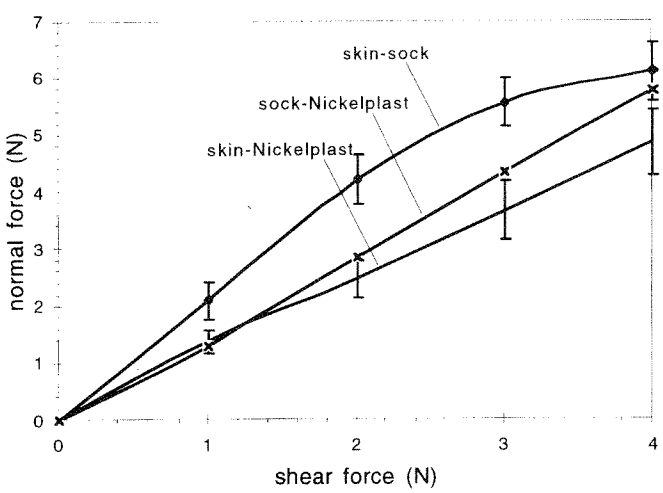

Figure 10.
Normal force vs. shear force data for different interfaces. Results for the skin-sock, sock-Nickelplast, and skin-Nickelplast interfaces are shown. For the skin-sock and skin-Nickelplast interfaces, the data represent the means for all subjects tested.

In general, COF values for the sock-material interface tests were lower than those for the skin-material interfaces. The only exception was Poron, where values at three of the four force levels were higher for the sock-material interface than that for the skin-material interface.

Table 9.
Frictional coefficients at the skin-sock interface.

Shear Force (N)	Skin-Sock
1	0.49 ± 0.08
2	0.48 ± 0.05
3	0.54 ± 0.04
4	0.66 ± 0.06
all force levels	0.53 ± 0.09

Mean±SD.

Skin-sock Interface

Results from the skin-sock interface show that shear force was nonlinearly related to normal force, similar to the cases for the skin-material and sock-material tests discussed above. COF values ranged from 0.48 (±0.05) to 0.66 (±0.06) for the different force levels (**Table 9**). The COF results at 1 N were significantly lower than those at 4 N. The COF results for the skin-sock interface were significantly less than those for the skin-material interface for all materials. Data from only the six subjects evaluated in both tests were used to make this comparison. As an example, results for Nickelplast are shown in **Figure 10.** Mean COF magnitudes for all materials together for each of the three interface configurations were: 0.75 (±0.11) for skin-material interfaces; 0.67 (±0.09) for sock-material interfaces; 0.53 (±0.09) for skin-sock interfaces.

DISCUSSION

Quantification of the compressive properties of interface materials and their COFs with skin and socks provides information of potential utility to the evaluation of interface material effects on interface pressures and shear stresses. The parameterized data reported here could be used with finite element (FE) models of residual limb-prosthetic socket systems or body-orthosis systems to assess interface pressure and shear stress sensitivity to CS and COF. A number of investigators have developed FE models of residual limb-prosthetic socket systems (20–27).

Compression Testing

Variability among samples of the same material in the compression testing data was likely due to variability in the material samples themselves, since errors in the compression testing system were relatively low. This variability is important because it potentially affects the degree of control on interface pressures and shear stresses one can achieve through the use of different liner materials.

These CS data are an extension of Campbell's efforts (1) in that here materials are classified based on a quantitative characterization of the complexity of their S-S curve rather than a qualitative assessment of shape. Further, in this study both nonrecovered and recovered strains were included. Campbell's three groups were: 1) a moderate-to-high initial slope followed by a plateau and then a steeper slope; 2) a low initial slope that increases with load; and 3) an approximately linear response. These correspond roughly to the groups presented here: 1) Group 1 materials: third-order polynomial fit; 2) Group 2 materials: second-order polynomial fit; and 3) Group 3 material: linear fit.

Choice of the material group depends on the application of interest and the desired material mechanical response. Group 1 materials, because they experience minimal nonrecovered strain, are appropriate in cases where a liner should maintain its thickness and volume after release from each cycle of loading. However, the relatively low stiffness intermediate regions in their S-S curves means that the materials do not become stiffer as stress is increased, but instead compress appreciably after the initial stages of loading before becoming more stiff at much higher stress levels. This intermediate stage may be appropriate in some applications but in others could cause a sense of instability to the user.

Group 2 materials experienced the greatest nonrecoverable strain of all materials. Thus, they change volume as cyclic loading is continued, a feature that needs to be accounted for in design if the volume enclosed within the liner is important, as in prosthetic applications for example. Group 2 materials become increasingly stiff with higher stresses, a feature similar to skin and connective tissue. A matching of material properties at soft tissue-body support interfaces can reduce stress concentrations at the interface. Our results demonstrate that Soft Pelite had a greater CS than Medium Pelite, a finding expected as a result of the excessive overloading of Soft Pelite in this study. Soft Pelite compressed to approximately 10 percent of its original thickness during the 60-min compression tests.

The Group 3 material was approximately linear, demonstrating the same CS at low and high stress levels. Linear materials are more predictable in terms of their mechanical response, though the high stiffness of the material tested here would suggest that it would not contribute an appreciable cushioning effect on soft tissues.

The changes in properties of the materials over the 60-min testing interval indicate a loss of thickness and air space within the materials over time. Slopes of the S-S curves generally increased over time, illustrating a loss of energy-absorbing capabilities, a feature that could affect the energy delivered to the soft tissues. For a given maximum stress level, a material with a steeper slope will be able to absorb less energy than one with a more shallow slope. Further, for prosthetic applications, the loss of thickness over repetitive cyclic loading alters the volume of the socket. A 1 mm reduction in material thickness corresponds to an approximately 4.2 percent volume change of the socket. This estimate was calculated based on a model of a transtibial residual limb of moderate size. Fernie suggests that residual limb volume changes outside of a −10 percent to +5 percent range can cause fit problems (28). Changes in material properties over time can have an important impact on residual limb-prosthetic socket interface mechanics.

It is important to note that the cyclic loading conducted here was over 10-min and 60-min time intervals, and all materials were new at the start of the tests. Conclusions about the performance of the materials over longer-term intervals cannot be made from the studies described here.

Friction Testing

The results suggest that the standard deviations in the friction data are more likely due to subject-to-subject variability than errors in the instrumentation. Though there was variability among subjects, there was not a consistent trend of one subject demonstrating higher COF values over other subjects for all materials.

The increase in COF at higher force levels is consistent with results presented by Comiash (14) between skin and sheet or knitted materials. It is possible that the higher forces caused fluid from the epidermis to be released, creating a stickier surface. However, it was also demonstrated here that COF for sock-material interfaces, where there is no epidermis, also demonstrated an increase in COF at higher force

levels. Thus, factors other than exclusively a biological one are important in influencing the nonlinear shear force-normal force relationship.

COF data for skin-material interfaces showed a dependence on the material groups (the groups were defined from compression testing data). The Group 1 materials generally had lower COFs and lower CS than the Group 2 and 3 closed-cell foam materials. However, the link is expected more as a result of the material surface characteristics than of their CS. Poron is an open-cell foam with a very smooth surface, while Spenco, though a rubber, is covered with a membrane of woven material.

The COF differences among the interfaces provide insight into where slip occurs in a residual limb-prosthetic socket system or limb-orthosis system. Because the COFs at the skin-sock interface were lower than those for the sock-material interfaces, slip would be expected at the skin surface rather than the sock-liner interface if a wool sock and liner were worn. Comparison of skin-sock results with skin-material results suggest that a higher COF would occur if no sock were present. The higher COF would be expected to affect the interface pressure and shear stress distribution. Other factors, however, such as the capability of the liner to absorb sweat might also affect COF. Comparison of results presented here with those reported in the literature for skin-polyethylene interfaces (13) demonstrate, in general, high COF values for the liner materials evaluated here.

COFs are important in prosthetics and orthotics applications because they influence pistoning as well as the distribution of pressures and shear stresses on the soft tissues. A low COF interface will result in slip, causing friction (shear force accompanied by displacement), a condition more likely to cause tissue trauma than a high COF no-slip case, assuming consistent interface stress magnitudes. However, slip also has advantages, for example, pistoning in prosthetics. Displacement between the residual limb and socket contributes to a pumping effect of the tissues and improved tissue perfusion. The prosthetic or orthotic designer can use the COF data presented here in a relative sense, gaining insight into the slip/stick performance of one material or interface over another. The data also provide quantitative information for FE modeling in prosthetics and orthotics, information that can be used to help provide insight into the influence of different design features on interface mechanics.

REFERENCES

1. Campbell G, Newell E, McLure M. Compression testing of foamed plastics and rubbers for use as orthotic shoe insoles. Prosthet Orthot Int 1982;6:48–52.
2. Campbell GJ, McLure M, Newell EN. Compressive behavior after simulated service conditions of some foamed materials intended as orthotic shoe insoles. J Rehabil Res Dev 1984;21(2):57–65.
3. Sanders JE, Daly CH. How does vacuum forming affect Pelite mechanical properties? Prosthet Orthot Int 1994;18:43–8.
4. Kuncir EJ, Wirta RW, Golbranson FL. Load-bearing characteristics of polyethylene foam: an examination of structural and compression properties. J Rehabil Res Dev 1990; 27(3):229–38.
5. Brodsky JW, Kourosh S, Stills M, Mooney V. Objective evaluation of insert material for diabetic and athletic footwear. Foot Ankle 1988;9(3):111–6.
6. Orders C. A comparison in medium and low density Plastazote in the fabrication of insoles. Can J Occup Ther 1977;45(1):17–8.
7. Strandberg L. Ergonomics applied to slipping accidents. In: Kvalseth TO, editor. Ergonomics of workstation design. London: Butterworths; 1983.
8. Chaffin DB, Woldstad JC, Trujillo A. Floor/shoe slip resistance measurement. Am Ind Hyg Assoc J 1992;53:283–9.
9. Perkins PJ, Wilson MP. Slip resistance testing of shoes: new developments. Ergonomics 1983;26(1):73–82.
10. Roberts AD, Thomas AG. Static friction of smooth clean vulcanised rubber. NR Tech 1976;7:38–42.
11. Ratner SB, Lavrentev VV. Evidence for the static friction of the unlubricated rubber. Doklady Akademii Nauk SSSR 1956;108:461–4. Research Association of British Rubber Manufacturers (now Rubber and Plastics Research Asssociation), Translation 591.
12. Andres RO, Chaffin DB. Ergonomics analysis of slip-resistance measurement devices. Ergonomics 1985;28(7): 1065–79.
13. Naylor PFD. The skin surface and friction. Br J Dermatol 1955;67:239–48.
14. Comaish S, Bottoms E. The skin and friction: deviations from Amonton's laws, and the effects of hydration and lubrication. Br J Dermatol 1971;84:37–43.
15. Elsner P, Wilhelm D, Maibach HI. Frictional properties of human forearm and vulvar skin: influence of age and correlation with transepidermal water loss and capacitance. Dermatologica 1990;181:88–91.
16. Cua AB, Wilhelm K-P, Maibach HI. Frictional properties of human skin: relation to age, sex and anatomical region, stratum corneum hydration and transepidermal water loss. Br J Dermatol 1990;123:473–9.
17. Highley KR, Coomey M, Den Beste M, Wolfram LJ. Frictional properties of skin. J Invest Dermatol 1977;69:303–5.
18. Sanders JE, Lam D, Dralle AJ, Okumura R. Interface pressures and shear stresses at thirteen socket sites on two persons with transtibial amputation. J Rehabil Res Dev 1997;34(1):19–43.

19. Sanders JE, Garbini JL, Leschen JM, Allen MS, Jorgensen JE. A bi-directional load applicator for the investigation of skin response to mechanical stress. IEEE Trans Biomed Eng 1997;44:290–6.
20. Brennan JM, Childress DS. Finite element and experimental investigation of above-knee amputee limb/prosthesis systems: a comparative study. 1991 Adv Bioeng, ASME WAM, 1991;BED-20:547–50.
21. Quesada P, Skinner HB. Analysis of a below-knee patellar-tendon-bearing prosthesis: a finite element study. J Rehabil Res Dev 1991;28(3):1–12.
22. Reynolds DP, Lord M. Interface load analysis for computer-aided design of below-knee prosthetic sockets. Med Biol Eng Comput 1992;30:419–26.
23. Sanders JE, Daly CH. Normal and shear stresses on a residual limb in a prosthetic socket during ambulation: comparison of finite element results with experimental measurement. J Rehabil Res Dev 1993;30(2):191–204.
24. Silver-Thorn MB, Childress DS. Parametric analysis using the finite element method to investigate prosthetic interface stresses for persons with trans-tibial amputation. J Rehabil Res Dev 1996;33(3):227–38.
25. Steege JW, Childress DS. Analysis of trans-tibial prosthetic gait using the finite element technique. Proceedings of the 21st Annual Meeting and Scientific Symposium, AAOP; 1995 Mar 21-25, New Orleans, LA; 1995. p. 13–4.
26. Zhang M, Lord M, Turner-Smith AR, Roberts VC. Development of a non-linear finite element modeling of the below-knee prosthetic socket interface. Med Eng Phys 1995:17(8):559–66.
27. Zhang M, Mak AF. A finite element analysis of the load transfer between an above-knee residual limb and its prosthetic socket: roles of interface friction and distal-end boundary conditions. IEEE Trans Rehabil Eng 1996;4(4):337–46.
28. Fernie GR, Holliday PJ. Volume fluctuations in the residual limbs of lower-limb amputees. Arch Phys Med Rehabil 1982;63:162–5.

Submitted for publication July 10, 1997. Accepted in revised form September 5, 1997.